International Journal of Science and Research Archive
eISSN: 2582-8185
Cross Ref DOI: 10.30574/ijsra
Journal homepage: https://ijsra.net/

(RESEARCH ARTICLE)

Check for updates

Explore the Impact of Dimensional Characteristics on the Thermal Behavior of Nanomaterials

Anod Kumar Singh [1], Reetesh Srivastava [2], Harish Chandra Srivastava [3], Brijesh Kumar Pandey [4] and Abhay P Srivastava [4,*]

[1] *Department of Humanities and Applied Science, School of Management Sciences, Lucknow, (UP), India.*
[2] *Department of Physics, Nandini Nagar P.G. College, Nawabganj, Gonda, (UP), India.*
[3] *Munna Lal Inter College, Wazirganj, budaun, (UP), India.*
[4] *Department of Applied Science and Humanities, Goel Institute of Technology and Management, Lucknow (UP), India.*

International Journal of Science and Research Archive, 2025, 17(03), 560-571

Publication history: Received on 08 November 2025; revised on 13 December 2025; accepted on 16 December 2025

Article DOI: https://doi.org/10.30574/ijsra.2025.17.3.3274

Abstract

This research explains how temperature acts in tiny particles, such as ZrO_2, Ag, ZnO, NiO, and Al, using some cool tools: the Dixit–Srivastava EOS, the Birch–Murnaghan EOS, and a heat-focused model. We're essentially using these models to predict how temperature changes as these nanoparticles expand, and then verifying if our predictions match real-world experiments. Turns out, the Dixit–Srivastava EOS usually nails it, giving us the most accurate forecasts for all the materials. Interestingly, metals seem to cool down faster due to their surface, but ionic oxides are tougher and hold onto their heat better. So, it seems these EOS models with nanoscale adjustments work well, and we can use this knowledge to create better nanomaterials for electronics, energy, and structures.

Keywords: Equation of state; Volume thermal expansion coefficient; Nanomaterials; Anderson-Gruneisen parameter; Bulk modulus

1. Introduction

In recent years, nanomaterials have garnered significant attention due to their distinct behavior compared to the same materials in their bulk form. As materials are made smaller, down to the scale of billionths of a meter (nanometers), their physical and chemical properties change. One crucial property strongly affected by size is how materials respond to temperature. For example, a metal nanoparticle may melt at a significantly lower temperature than the same metal in bulk form. These changes are mainly due to the large number of atoms on the surface of nanoparticles, which behave differently from atoms inside the material [1-3].

This study investigates the impact of size on temperature-dependent characteristics across five distinct nanomaterials: zirconium dioxide (ZrO_2), silver (Ag), zinc oxide (ZnO), nickel oxide (NiO), and aluminum (Al). These materials were selected for their widespread use in industries, including electronics, energy, sensors, and coatings. While each possesses unique attributes, a common thread is the alteration in behavior as particle size diminishes to the nanoscale [4-6].

Nano-sized zirconium dioxide (ZrO_2), for instance, is celebrated for its notable strength and impressive heat resistance, along with stability under demanding conditions. ZrO_2 can assume various crystal structures, influenced by both temperature and particle dimensions, thereby boosting its adaptability. Thanks to its toughness and resistance to wear,

* Corresponding author: Abhay P Srivastava

nano ZrO_2 finds extensive use in producing robust ceramics, dental implants, and even cutting tools. The capacity to conduct oxygen ions at elevated temperatures makes it vital in fuel cells and oxygen sensors [7-8].

Silver (Ag) nanoparticles are particularly well-known for their potent antibacterial and antiviral effects. They also boast exceptional electrical and thermal conductivity, rendering them suitable for electronic device applications. Nano-silver is employed in medical coatings, wound dressings, and water filters due to its ability to combat harmful microbes. Owing to its optical and electrical attributes, silver is also finding its way into flexible electronics, conductive inks, and specific solar cell technologies [9-10].

In its nanoscale form, zinc oxide (ZnO) is a versatile material. Nano ZnO exhibits notable ultraviolet (UV) absorption, photocatalytic action, and antibacterial qualities. As a consequence, it is commonly included in sunscreens, skincare formulations, and protective coatings. It is also utilized in sensors, LED lighting solutions, and applications aimed at environmental remediation, notably for the breakdown of pollutants using sunlight. Its semiconducting traits also make it useful in electronics and optoelectronics [11-12].

Nickel oxide (NiO) nanoparticles are recognized for their thermal stability, magnetic behavior, and function as p-type semiconductors. Because of these characteristics, NiO is an important material in battery technology, notably as an electrode component within lithium-ion batteries. It is also used in smart windows (electrochromic devices), gas sensors, and supercapacitors. The material is appreciated for its efficiency in storing and moving charge [13-14].

Aluminum (Al) nanoparticles are lightweight and demonstrate heightened reactivity due to their significant surface area. Although reactive, they tend to develop a protective oxide layer that inhibits corrosion. Nano-aluminum finds widespread application in energetic materials like propellants and explosives because it liberates substantial energy upon combustion. Applications are lightweight structural components, electronics, and water treatment and hydrogen production applications because of its reducing properties [15].

Comprehending the temperature-size relationship in these materials is key to enhancing their functionality in practical scenarios. To illustrate, if a substance melts or displays instability at a lower temperature due to its diminutive size, it might prove unsuitable for uses requiring high temperatures. Conversely, some property alterations might be advantageous, such as enhanced thermal conductivity or heightened reactivity [16].

\Through the examination and comparison of these five nanomaterials, this research seeks to improve our grasp of how size influences temperature-related performance, and to deliver insightful information for scientists and engineers engaged in nanotechnology across diverse domains.

2. Methodology:

The thermal pressure of the solid can be expressed as [17]:

$$P_{th} = \int_{T_0}^{T} \alpha K dT \qquad \ldots\ldots\ldots \qquad (1)$$

Where α is the thermal expansion coefficient, and K is bulk modulus.

At the zero-pressure equation, (1) can be written as:

$$P_{th} = \int_{T_0}^{T} \alpha_0 K_0 dT \qquad \ldots\ldots\ldots \qquad (2)$$

Where α_0 is the volume thermal expansion coefficient, and K_0 is the bulk modulus at zero pressure.

Integrating equation (2) gives the following relation.

$$P_{th} = \alpha_0 K_0 (T - T_0) \qquad \ldots\ldots\ldots\ldots \qquad (3)$$

By leveraging the principles of finite strain theory, we utilize the Birch-Murnaghan equation [19] and the Dixit-Srivastava equation of state [18]. This approach enables us to study the complex pressure-volume-temperature relationship, ultimately providing insights into material behavior across temperatures. The Dixit-Srivastava and Birch-Murnaghan equation of state can be expressed as:

$$P_{D-S} = \frac{6}{7}K_0\left[\left(\frac{V}{V_0}\right)^{-10/3} - \left(\frac{V}{V_0}\right)^{-13/6}\right] + \frac{54}{882}K_0\left(K_0^{'}+1\right)\left[\left(\frac{V}{V_0}\right)^{-9/2} - 2\left(\frac{V}{V_0}\right)^{-10/3} + \left(\frac{V}{V_0}\right)^{-13/6}\right] \quad \ldots\ldots \quad (4)$$

$$P_{B-M} = \frac{3}{2}K_0\left[\left(\frac{V}{V_0}\right)^{-7/3} - \left(\frac{V}{V_0}\right)^{-5/3}\right] \times \left[1 + \frac{3}{4}\left(K_0^{'}-4\right)\left\{\left(\frac{V}{V_0}\right)^{-2/3} - 1\right\}\right] \quad \ldots\ldots \quad (5)$$

Equations (4) and (5) are isothermal equations of state, which do not include the effect of temperature. To make a complete equation of state, we include the effect of temperature in equations (4) and (5). Thus, equations (4) and (5) may be rewritten as follows by taking $K_0^{'} = -1$ in equation (4) and $K_0^{'} = 4$ in equation (5).

$$P_{D-S} = \frac{6}{7}K_0\left[\left(\frac{V}{V_0}\right)^{-10/3} - \left(\frac{V}{V_0}\right)^{-13/6}\right] + P_{th} \quad \ldots\ldots \quad (6)$$

$$P_{B-M} = \frac{3}{2}K_0\left[\left(\frac{V}{V_0}\right)^{-7/3} - \left(\frac{V}{V_0}\right)^{-5/3}\right] + P_{th} \quad \ldots\ldots \quad (7)$$

Combining equations (3) and (6), we get the following relation:

$$P_{D-S} = \frac{6}{7}K_0\left[\left(\frac{V}{V_0}\right)^{-10/3} - \left(\frac{V}{V_0}\right)^{-13/6}\right] + \alpha_0 K_0(T - T_0) \quad \ldots\ldots\ldots \quad (8)$$

At P_{D-S} =0, equation (8) takes the following form

$$T_{D-S} = T_0 + \frac{6}{7\alpha_0}\left[\left(\frac{V}{V_0}\right)^{-13/6} - \left(\frac{V}{V_0}\right)^{-10/3}\right] \quad \ldots\ldots\ldots \quad (9)$$

The expression corresponding to the Birch-Murnaghan equation of state takes the following form.

$$T_{B-M} = T_0 + \frac{3}{2\alpha_0}\left[\left(\frac{V}{V_0}\right)^{-5/3} - \left(\frac{V}{V_0}\right)^{-7/3}\right] \quad \ldots\ldots\ldots \quad (10)$$

The coefficient of thermal volume expansion as a function of temperature can be expressed as [20]:

$$\alpha = a + bT + cT^2 + \ldots\ldots\ldots\ldots\ldots\ldots\infty \quad (11)$$

or

$$\alpha = \alpha_0 + \alpha_0^{'}(T - T_0) + \alpha_0^{''}(T - T_0)^2 + \ldots\ldots\ldots\ldots\ldots\ldots\infty \quad (12)$$

Where $\alpha_0^{'}$, $\alpha_0^{''}$ the first, second, and subsequent derivatives of temperature at zero pressure are defined at the initial condition. The equations are expressed in terms of these derivatives, as outlined in [21], with reference to [20].

$$\alpha_0^{'} = \alpha_0^2 \delta_T = \alpha_0^2 K_0^{'} \quad \text{.....} \quad (13)$$

$$\alpha_0^{'''} = \alpha_0^3 \delta_T^2 = \alpha_0^3 K_0^{'2} \quad \text{.....} \quad (15)$$

Where δ_T is the Anderson-Anderson-Gruneisen parameter. Now, equation (12) may be rewritten as:

$$\alpha = \alpha_0 + \alpha_0^2 K_0^{'}(T - T_0) + \alpha_0^3 K_0^2 (T - T_0)^2 + \text{.....}\infty \quad (16)$$

or

$$\frac{\alpha}{\alpha_0} = [1 - \alpha_0 K_0^{'}(T - T_0)]^{-1} \quad \text{.....} \quad (17)$$

According to Hu et al. [22], the relation between the volume thermal expansion coefficient and compression is written as:

$$\frac{\alpha}{\alpha_0} = \left(\frac{V}{V_0}\right)^{\delta_T} = \left(\frac{V}{V_0}\right)^{K_0^{'}} \quad \text{.....} \quad (18)$$

Combining equations (17) and (18), we get a thermodynamic formula for the size-dependent temperature of nanomaterials as:

$$T = T_0 + \frac{1}{\alpha_0 K_0^{'}}\left[1 - \left(\frac{V}{V_0}\right)^{-K_0^{'}}\right] \quad \text{.....} \quad (19)$$

Using equations (9), (10), and (19), we can estimate the size-dependent temperature of nanomaterials.

Table 1 Values of input parameters used in the present work with their references

Nanomaterial	K_0'	$\alpha_0 \times 10^{-5} K^{-1}$
ZrO_2	4.3 [23]	3.46 [28]
Ag	4 [24]	1.8 [29]
ZnO	4 [25]	1.04 [30]
NiO	4 [26]	3.77 [31]
Al	4 [27]	7.8 [32]

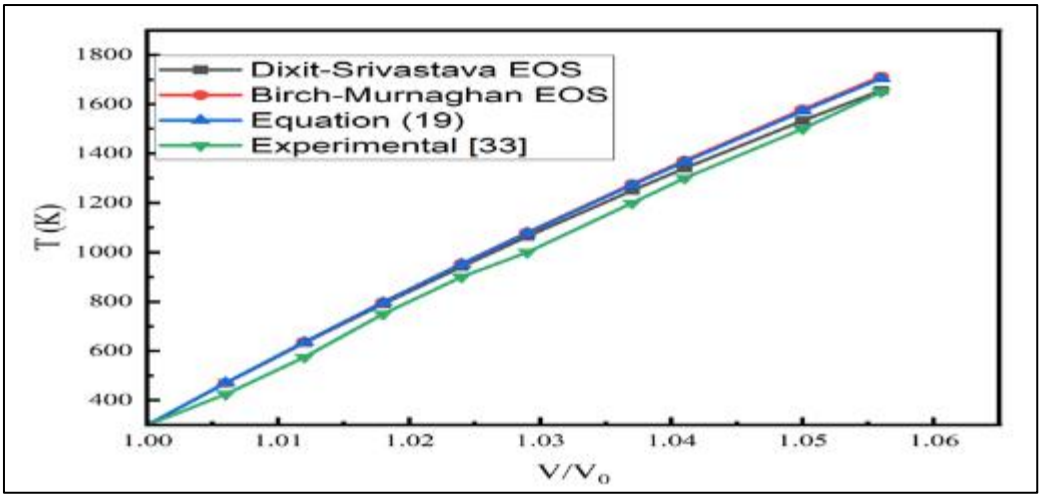

Figure 1 Variation of size-dependent temperature of ZrO_2

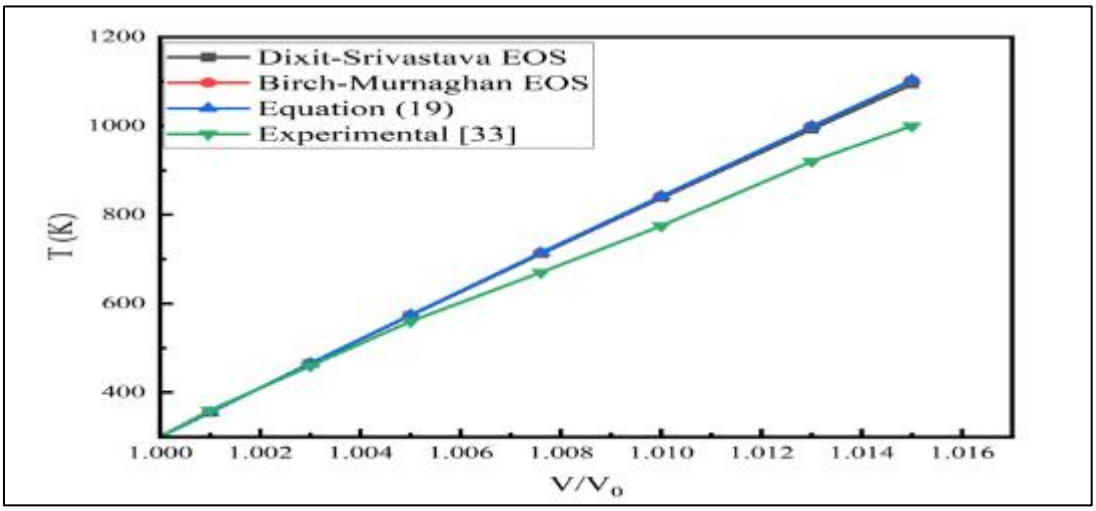

Figure 2 Variation of size-dependent temperature of Ag

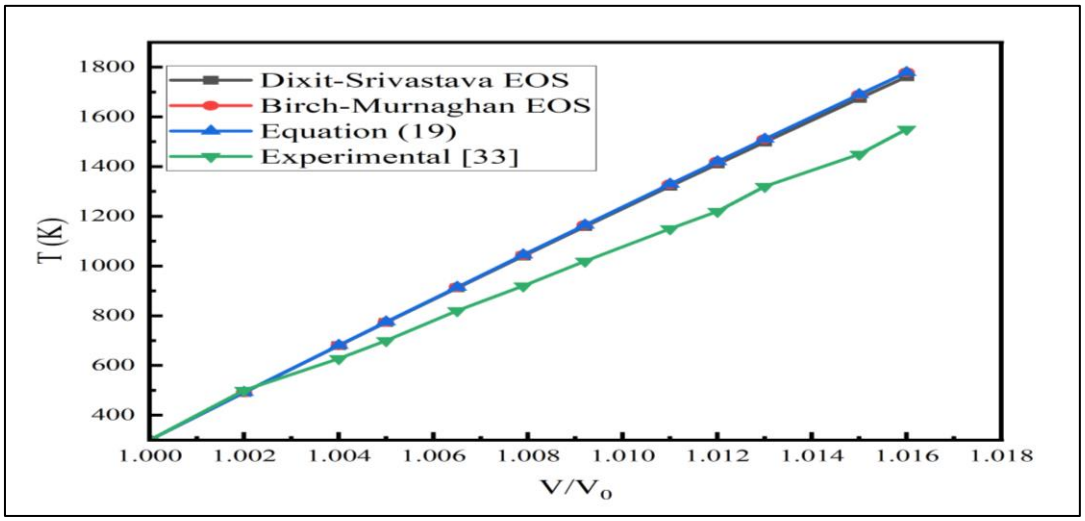

Figure 3 Variation of size-dependent temperature of ZnO

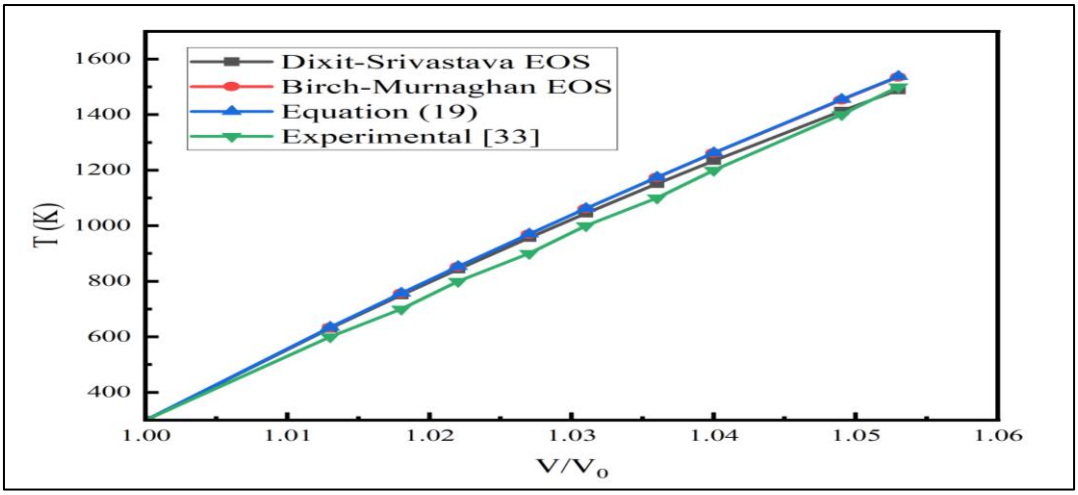

Figure 4 Variation of size-dependent temperature of NiO

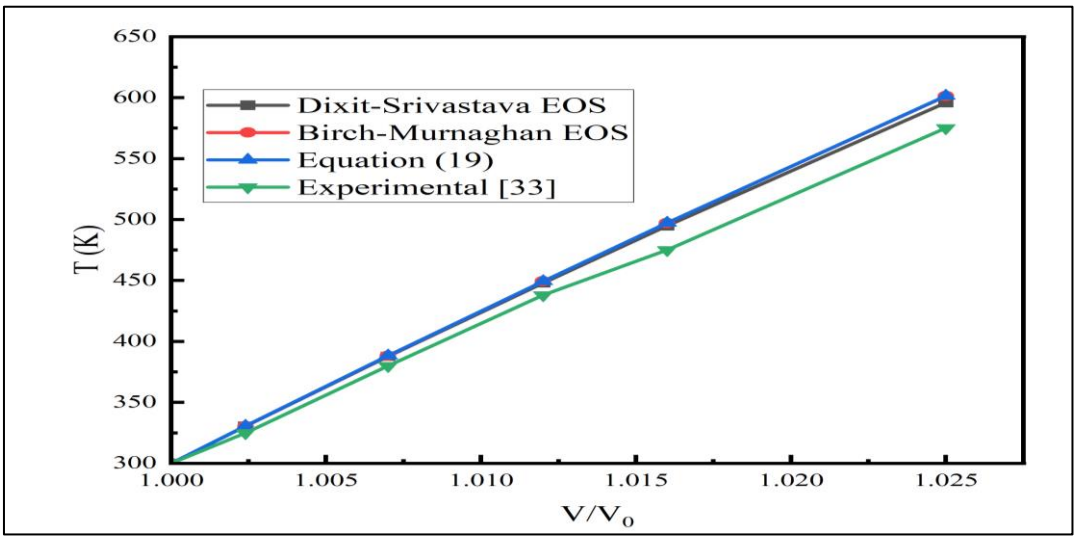

Figure 5 Variation of size-dependent temperature of Al

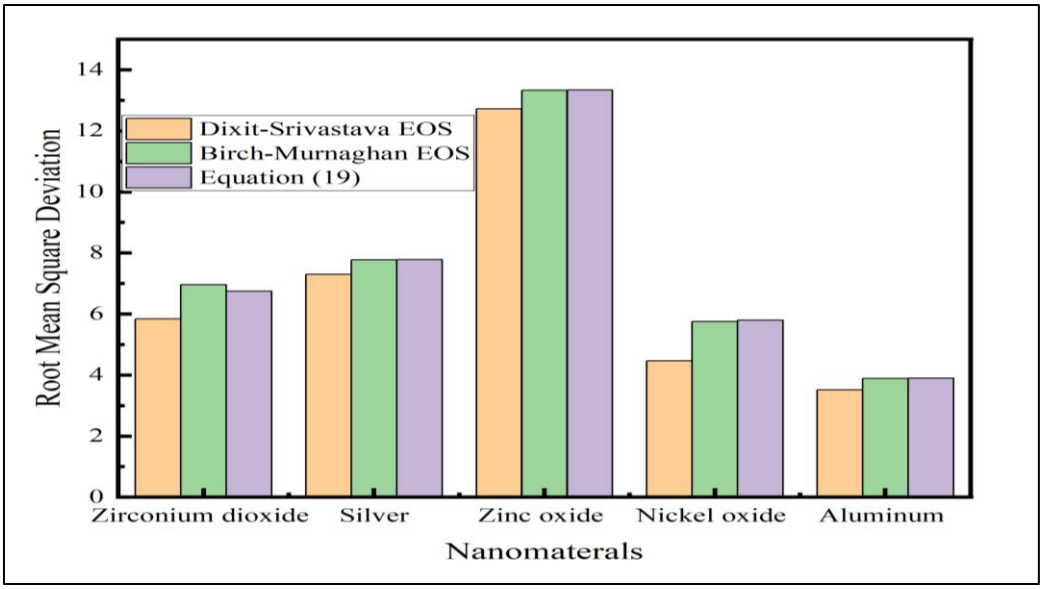

Figure 6 Root mean square deviation of different models

3. Result and Discussion

The input values used in this study are listed in Table 1. The curve between compression and temperature is shown in Figures 1-5 for different nanomaterials. Draw the curve between the root mean square deviation for different nanomaterials shown in Figure 6 for better clarity and analysis.

Examine Figure 1, we can see how the temperature of ZrO_2 changes with size, plotted against how much its volume expands (V/V_0). Temperature (T, measured in Kelvin) is on the vertical axis, while the horizontal axis shows the volume change compared to its normal state. There are four different sets of data: Dixit–Srivastava EOS (marked with black squares), Birch–Murnaghan EOS (red circles), results from thermodynamic Equation (19) (blue triangles), and actual experimental measurements (green diamonds).

The trend is pretty linear; as the volume increases ($V/V_0 > 1.0$), the temperature also climbs steadily. This illustrates the strong connection between how ZrO_2 expands with heat and its temperature. When the volume is at its normal point ($V/V_0 = 1.0$), the models all meet at a low-temperature starting point. As the material expands, the curves rise almost in tandem, suggesting that the EOS formulations are reasonably accurate in describing the thermophysical behavior of ZrO_2.

It's worth noting that the Dixit–Srivastava EOS is the closest to the experimental data across the board, with only a minor difference appearing at larger expansions. The Birch–Murnaghan EOS, on the other hand, tends to overestimate the temperature at higher volumes, probably due to its limitations in capturing specific nanoscale effects. Equation (19), derived from thermodynamic principles, falls between these two but still tends to run slightly higher than the experimental data. The experimental curve stays lower than the predicted values when expansion is greater, and this can probably be attributed to real-world things such as surface disorder, the formation of oxygen vacancies, and the grain boundary impacts that aren't completely represented in the EOS models.

In most cases, this graph underlines two essential things: firstly, ZrO_2 displays a predictable, consistent rise in size-related temperature as its volume expands, which is thanks to its strong ionic–covalent bonds; and secondly, the Dixit–Srivastava EOS appears to offer the most accurate agreement quantitatively, demonstrating its usefulness in modeling how ceramic oxides behave thermally at the nanoscale.

Figure 2 illustrates how the temperature of Ag changes with normalized volume expansion (V/V_0). The y-axis represents temperature (T, measured in Kelvin), while the x-axis displays the ratio of expanded volume to the equilibrium volume. Comparing the data, theoretical predictions using the Dixit–Srivastava EOS (black squares), the Birch–Murnaghan EOS (red circles), and thermodynamic Equation (19) (blue triangles) are plotted against experimental findings (green diamonds).

While the trend generally indicates a linear rise in temperature alongside volume expansion, unlike ZrO_2, silver exhibits a more notable divergence between theoretical expectations and the actual data as expansion progresses. Near V/V_0 = 1.0, the models largely converge with the experiment, suggesting that the EOS formulations adequately represent the initial thermal behavior. However, past V/V_0 = 1.006, the theoretical curves tend to predict higher temperatures compared to the measured values. This could imply that small metallic Ag nanoparticles experience more intense surface-related phenomena and augmented anharmonic vibrations that the basic EOS may not completely account for.

Interestingly, the Dixit–Srivastava EOS shows marginally better initial agreement with experimental data than the Birch–Murnaghan EOS in the low expansion range. Yet, both models ultimately deviate at higher expansion levels. Thermodynamic Equation (19) generally mirrors the EOS-based estimations, but tends to overestimate the experimental curve. Across the volume expansion range, the experimental results consistently show lower temperatures, possibly resulting from substantial surface-to-volume ratio effects and adsorbate interactions, which collectively diminish the effective binding energy and reduce the temperature beyond what is predicted by simplified models.

Overall, this figure emphasizes that silver nanoparticles, owing to their metallic bonding and lower cohesive energy, demonstrate more pronounced size-dependent temperature depression than oxides. Furthermore, it highlights the need to consider surface reconstructions and electron–phonon interactions to create more accurate predictive models. Though the Dixit–Srivastava EOS provides an adequate estimation, further enhancements are needed to describe the sharp experimental variations as expansion increases fully.

Figure 3 illustrates how the temperature of ZnO nanoparticles changes relative to their normalized volume expansion (V/V_0). On the vertical axis, we will find temperature (T) measured in Kelvin, while the horizontal axis represents the relative expansion compared to the equilibrium volume. We're comparing theoretical predictions—Dixit–Srivastava EOS (black squares), Birch–Murnaghan EOS (red circles), and Equation (19) (blue triangles)—against actual experimental data (green diamonds).

The temperature increases linearly as the nanoparticles expand, which aligns with what we expected for ZnO under nanoscale thermal conditions. Near V/V_0 = 1.0, the theoretical predictions and experimental data match pretty well. This suggests that the EOS models accurately represent the initial thermophysical response. However, it's worth noting that as the expansion increases, the experimental values tend to be lower than the theoretical curves. This difference likely stems from defects in the ZnO nanoparticles, such as oxygen vacancies and surface reconstructions, which weaken the binding strength and thus lower the experimental temperatures.

Suppose we see the theoretical models, the Dixit–Srivastava EOS and the Birch–Murnaghan EOS give almost identical predictions. Equation (19) tends to overestimate compared to the other two slightly, but the overall trend remains consistent. Despite their similarities, all three theoretical models overestimate the experimental results at larger expansions. This highlights a limitation: they don't fully account for defect chemistry and surface energetics at the nanoscale.

Physically, this figure shows that ZnO's behavior falls somewhere between metallic systems like silver (Ag) and strongly ionic oxides like zirconia (ZrO_2) and nickel oxide (NiO). Its covalent-ionic bonding provides some structural stability, but its polar surfaces and sensitivity to oxygen-related defects make it more susceptible to nanoscale effects than zirconia or nickel oxide. The fact that experimental results are systematically lower than theoretical predictions emphasizes how much surface states and lattice imperfections control the thermal response at this scale. While the Dixit–Srivastava EOS is perhaps the most accurate model, it still requires refinement to capture the defect-driven thermal behavior of ZnO nanoparticles fully.

The curve 4 details how temperature changes with size for NiO relative to volume expansion (V/V_0). Temperature (T in Kelvin) is on the Y-axis, while the X-axis indicates how much the volume has expanded compared to its original. The plot compares what we'd expect from the Dixit–Srivastava EOS (black squares), the Birch–Murnaghan EOS (red circles), and, notably, Equation (19) (blue triangles) with actual lab measurements (green diamonds).

Temperature increases in an almost straight line as the volume expands, which is what we'd anticipate thermodynamically for NiO when it's compressed or expanded. Near V/V_0 = 1, the theoretical predictions and experimental values match closely, showing these methods effectively model behavior at low expansion. However, the lab measurements don't climb as fast as the theoretical curves as expansion continues, leading to a small divergence at larger volumes. This hints at the effects of nanoscale properties, like missing oxygen or nickel atoms, which can weaken the structure and lower the temperature response.

Once again, the Dixit–Srivastava EOS is closest to what we see experimentally, with the Birch–Murnaghan EOS slightly overshooting temperature at higher expansions. Equation (19) behaves similarly, but its values are consistently a bit higher than the EOS models. The models' relatively minor deviations from the lab data suggest NiO, a strongly ionic oxide with stable rock-salt bonds, is less prone to surface issues than metals like Ag or Al, and even less sensitive to defects than ZnO, known for its polar surfaces.

In summary, this figure underscores the thermal stability of NiO nanoparticles, where observed deviations from theory remain relatively modest, unlike some other materials. This robust ionic bonding seems to help maintain a bulk-like thermal response even at the nanoscale, although vacancy-related disorder still explains why experimental values are somewhat underestimated. Overall, the Dixit–Srivastava EOS remains the best for modeling NiO's nanoscale behavior, reaffirming its effectiveness for strongly ionic oxides.

Let's examine the figure 5, how the size-dependent temperature of aluminum nanoparticles varies with normalized volume expansion (V/V_0). The plot illustrates this, with temperature (T, in Kelvin) on the vertical axis and the volume expansion ratio on the horizontal. We see predictions from the Dixit–Srivastava EOS (black squares), alongside those of the Birch–Murnaghan EOS (red circles), and also Equation (19) (blue triangles), all compared against actual experimental data (green diamonds).

The temperature increases as V/V_0 gets larger, displaying a nearly linear relationship – thus, expansion seems to boost the thermal response directly. Near $V/V_0 = 1.0$, the models tend to align well with the experiment. This suggests our theoretical frameworks reasonably capture the initial thermal behavior of aluminum under near-equilibrium states. But interestingly, as expansion grows, the theoretical predictions and experimental curve begin to separate, calculated values becoming, in most cases, noticeably higher. This difference is noticeable beyond $V/V_0 > 1.015$, with the experimental curve staying below the model outputs.

This divergence may stem from the distinct properties inherent to aluminum nanoparticles. Aluminum, a metal with relatively weak cohesive energy, demonstrates significant size-dependent temperature depression. However, unlike silver (Ag), aluminum naturally forms a stabilizing, protective oxide shell. This passivation dampens surface disorder, slightly reducing the effective temperature depression, which can cause disparities between actual measured data and simplified theoretical results. The models, in their current form, don't entirely account for this oxide shell effect, and as a result, tend to overestimate the size-dependent temperature slightly. Notably, the Dixit–Srivastava EOS appears to perform relatively better, following the experimental trend somewhat more closely, although it also slightly overestimates at higher expansions. The Birch-Murnaghan EOS aligns quite closely with Equation (19), although it seems to exaggerate the upward trend compared to the experimental data slightly. Ultimately, aluminum nanoparticles demonstrate a specific equilibrium between metallic bonding and the stabilizing influence of the oxide shell. The metallic characteristics, in particular, lead to considerable thermal sensitivity when dimensions are reduced. However, the presence of an oxide shell helps moderate this somewhat, leading to a more rapid convergence towards bulk-like values when compared to, say, silver. The theoretical predictions exhibit reasonable accuracy at lower expansions but require more careful calibration to fully address the surface oxidation and passivation processes at play on the nanoscale.

Figure 6 presents a comparative analysis of root mean square deviation (RMSD) values, illustrating that three theoretical models predict the temperature behavior of several nanomaterials. Now, when we examine materials like zirconium dioxide, we tend to see is that the Dixit–Srivastava EOS generally gives us the lowest RMSD. This suggests that it could be particularly useful for understanding the thermal behavior observed in this strongly ionic material. Equation (19) and the Birch–Murnaghan EOS, on the other hand, often show larger deviations. This suggests they might be less effective when it comes to accurately reproducing the behavior observed in ZrO_2. However, silver is a different story, as all three models yield higher RMSD values than the oxides, even though the Dixit–Srivastava EOS still manages to edge out the others slightly. This could be because modelling metallic systems is frequently more complex, perhaps due to surface effects and melting point depression – aspects not always fully accounted for in conventional EOS frameworks. A lower RMSD, of course, means a better fit between predictions and the experimental data. We're considering the Dixit–Srivastava EOS (orange), the Birch–Murnaghan EOS (green), and Equation (19) (purple) applied to Al, Ag, NiO, ZnO, and ZrO_2. Interestingly, zinc oxide exhibits the highest RMSD values, regardless of which model is used. This emphasizes just how sensitive ZnO is to nanoscale phenomena, such as polar surface terminations, oxygen vacancies, and reconstructions caused by defects – all of which can significantly impact its thermal behavior. These effects, however, aren't always adequately accounted for in these theoretical models. Nickel oxide, on the other hand, exhibits moderate RMSD values, with the Dixit–Srivastava EOS again providing the best accuracy. The relatively small deviations across models, in most cases, imply that NiO's strong ionic bonds make it less susceptible to disorder at the nanoscale, especially when compared to ZnO or metallic systems. As for aluminum, it displays the lowest RMSD across

all three models, which might be attributed to the stabilizing role of its natural oxide shell, which in turn could reduce thermal fluctuations, allowing the models to reproduce its behavior with reasonable accuracy.

In summary, the figure tends to demonstrate that the Dixit–Srivastava EOS frequently achieves the lowest RMSD, or close to it, across these materials. This reinforces its enhanced ability to predict compared to the Birch–Murnaghan EOS and Equation (19). However, the exceptionally high RMSD for ZnO highlights that models that explicitly consider defect chemistry and surface energetics are likely needed to match experimental trends accurately. This comparative analysis validates the Dixit–Srivastava EOS as a relatively reliable framework for predicting thermal behavior at the nanoscale, while also underscoring the inherent limitations of all three approaches when dealing with materials exhibiting substantial defect or surface-related effects.

4. Conclusion

It's clear from this work that particle size is a significant factor when it comes to how nanomaterials react to heat. In all the systems we looked at – five in total – temperature went up steadily as they expanded. However, just how much they strayed from what we expect from the bulk material really hinged on factors such as the strength of the bonds between atoms and what was happening on the surface. Zirconia (ZrO_2) and nickel oxide (NiO), for instance, were pretty stable because they have strong ionic bonds. On the other hand, silver (Ag) and aluminum (Al) experienced larger drops in temperature, likely because they have metallic bonds and a large surface area compared to their volume. Zinc oxide (ZnO) was the most interesting case; its polar surfaces and oxygen defects led to some significant differences between what we saw and what theory predicted. This highlights that standard equations of state (EOS) aren't perfect when dealing with the quirky chemistry of nanoscale defects. Of the models we tested, the Dixit–Srivastava EOS generally gave the best results, consistently beating the Birch–Murnaghan EOS and the standard thermodynamic equation. It had the lowest RMSD values for all materials, making it a reliable method for predicting how nanomaterials behave when heated. Our findings really emphasize that if we want to predict the thermal behavior of nanomaterials accurately, we need to include corrections that account for their nanoscale properties. This knowledge could help design better nanomaterials for applications such as coatings, sensors, electronics, and energy technology.

Compliance with ethical standards

Disclosure of conflict of interest

The authors of this paper declare that they have no known financial interests or personal relationships that could have potentially influenced the work presented in this report.

Statement of ethical approval

The authors confirm that the manuscript is their original work and has not been previously published elsewhere.

Author's Contribution:

All authors contributed to the creation of the research outline.

Funding:

The authors state that they have no funding agencies available.

Availability of data and Materials:

The information used to support the study's conclusions is cited in the references and is publicly accessible.

References

[1] Srivastava, A. Prakash, Pandey, B. Kumar, Singh, A. Kumar, Srivastava, R., and Srivastava, H. Chandra (2025). Assessment of Several Equations of State for the Calculation of Thermodynamic Coefficients of Solids. Physical Chemistry Research, 13(4), 669-676. https://doi.org/10.22036/pcr.2025.524577.2685.

[2] Ibrahim Khan, Khalid Saeed, Idrees Khan, Nanoparticles: Properties, applications and toxicities, Arabian Journal of Chemistry, 12(7), 2019, 908-931, https://doi.org/10.1016/j.arabjc.2017.05.011.

[3] Srivastava, A.P., Pandey, B.K. & Pandey, A.K. Introducing an Innovative Exponential-Logarithmic Equation of State for Solids at High Compression: HCP Iron Exemplifies This Groundbreaking Advancement. Natl. Acad. Sci. Lett. (2025). https://doi.org/10.1007/s40009-025-01726-y.

[4] Haider, A., Ikram, M., Rafiq, A. (2023). Properties of Nanomaterials. In: Green Nanomaterials as Potential Antimicrobials. Springer, Cham. https://doi.org/10.1007/978-3-031-18720-9_3.

[5] Abhay. P. Srivastava, B.K. Pandey, A. K. Gupta, et al. The Relevance of the New Exponential Equation of State for Semiconductors. Iran J Sci 48, 1067–1074 (2024). https://doi.org/10.1007/s40995-024-01657-1.

[6] Srivastava, A.P., Pandey, B.K., Gupta, A.K. et al. Theoretical prediction of thermoelastic properties of bismuth ferrite by a new approach. J Math Chem 62, 2253–2264 (2024). https://doi.org/10.1007/s10910-024-01647-z .

[7] Abhay P. Srivastava, Brijesh K. Pandey, Abhishek Kumar Gupta, Calculation of the melting curve of metals using equations of state and Lindemann's law, Computational Condensed Matter, 42, 2025,e00986, https://doi.org/10.1016/j.cocom.2024.e00986.

[8] Aman K. Chitoria, Arshid Mir, M.A. Shah, A review of ZrO2 nanoparticles applications and recent advancements, Ceramics International, 49(20), 2023, 32343-32358, https://doi.org/10.1016/j.ceramint.2023.06.296.

[9] Abhay P. Srivastava, Brijesh K. Pandey, Abhishek K. Gupta, Explore the fascinating realm of comparing metal melting curves by applying the equation of state and Lindemann's law,Computational Condensed Matter, 40, 2024,e00952, 2352-2143, https://doi.org/10.1016/j.cocom.2024.e00952.

[10] Atanda, S.A., Shaibu, R.O. & Agunbiade, F.O. Nanoparticles in agriculture: balancing food security and environmental sustainability. Discov Agric 3, 26 (2025). https://doi.org/10.1007/s44279-025-00159-x .

[11] Abhay. P. Srivastava, B.K. Pandey, A. K. Gupta, et al. Comparing Melting Curves of Metals Using the Equation of State and Lindemann's Law. Iran J Sci (2024). https://doi.org/10.1007/s40995-024-01748-z.

[12] Thounaojam, T.C., Meetei, T.T., Devi, Y.B. et al. Zinc oxide nanoparticles (ZnO-NPs): a promising nanoparticle in renovating plant science. Acta Physiol Plant 43, 136 (2021). https://doi.org/10.1007/s11738-021-03307-0 .

[13] Abhay. P. Srivastava, B.K. Pandey, A constructive approach to formulating pressure-dependent binding energy using the equation of state. Ionics (2025). https://doi.org/10.1007/s11581-025-06183-7.

[14] Shilpa Thakur, Isha Thakur, Rajender Kumar, A review on synthesized NiO nanoparticles and their utilization for environmental remediation, Inorganic Chemistry Communications, 172, 2025,113758, https://doi.org/10.1016/j.inoche.2024.113758.

[15] Abhay. P. Srivastava, B. K. Pandey, & M. Upadhyay, (2024). Anticipating Pressure Changes in Halides under Compression. East European Journal of Physics, (3), 333-339. https://doi.org/10.26565/2312-4334-2024-3-37.

[16] Borode, A., Tshephe, T., Olubambi, P. et al. Effects of temperature and nanoparticle mixing ratio on the thermophysical properties of GNP–Fe2O3 hybrid nanofluids: an experimental study with RSM and ANN modeling. J Therm Anal Calorim 149, 5059–5083 (2024). https://doi.org/10.1007/s10973-024-13029-3 .

[17] M. Goyal, "Melting temperature of metals under pressure," Chinese J. Phys., vol. 66, pp. 453–460, 2020, https://doi.org/10.1016/j.cjph.2020.05.002.

[18] Chandra K. Dixit, Shivam Srivastava, Prachi Singh, Anjani K. Pandey, Analysis of finite strain theory for modeling a new EOS for nanomaterials, Nano-Structures & Nano-Objects, 38, 2024, 101121, https://doi.org/10.1016/j.nanoso.2024.101121.

[19] Qing He, Zu-Tong Yan, Study of Temperature Dependence of Bulk Modulus and Interatomic Separation for Ionic Solids, Physica Status Solidi B, 223, 767, 2001, https://doi.org/10.1002/1521-3951(200102)223:3<767::AID-PSSB767>3.0.CO;2-X.

[20] Yi Hu, H.-L. Tsai, C.-L. Huang, Effect of brookite phase on the anatase–rutile transition in titania nanoparticles, Journal of the European Ceramic Society, 23(5), 2003, 691-696, https://doi.org/10.1016/S0955-2219(02)00194-2.

[21] Lei Jin, Liyong Ni, Qinghe Yu, Abdul Rauf, Chungen Zhou, Theoretical calculations of thermodynamic properties of tetragonal ZrO2, Computational Materials Science, 65, 2012, 170-174, https://doi.org/10.1016/j.commatsci.2012.07.008.

[22] A. M. Alsheikh, A. A. Issa, Theoretical study of bulk and nanomaterials under high pressure, AIP Conf. Proc. 2213, 020099 (2020), https://doi.org/10.1063/5.0000247.

[23] Duzynska, A., Hrubiak, R., Drozd, V., Teisseyre, H., Paszkowicz, W., Reszka, A., … Suchocki, A. (2012). The structural and optical properties of ZnO bulk and nanocrystals under high pressure. High Pressure Research, 32(3), 354–363. https://doi.org/10.1080/08957959.2012.700308 .

[24] Khan, M. Z. R., & Ahmad, R. (2006). A Theoretical Calculation of the First Equilibrium Pressure Derivative of the Bulk Modulus, K_0' Using the Born–Mayer Theory. Material Science Research India, 3(2a), http://dx.doi.org/10.13005/msri/032a16.

[25] Abhay P. Srivastava, Brijesh K. Pandey, Abhishek K. Gupta, Explore the fascinating realm of comparing metal melting curves by applying the equation of state and Lindemann's law, Computational Condensed Matter, 40,2024, e00952, https://doi.org/10.1016/j.cocom.2024.e00952.

[26] Plummer, W.A., Gulati, S.T. (1982). Measurement of Thermal Expansion and Volume Changes in Partially Stabilized Zirconia. In: Larsen, D.C. (eds) Thermal Expansion 7. Springer, Boston, MA. https://doi.org/10.1007/978-1-4684-8267-6_1.

[27] Y Hu, H.-L Tsai, C.-L Huang, Phase transformation of precipitated TiO2 nanoparticles,Materials Science and Engineering: A,344(1), 2003,209-214, https://doi.org/10.1016/S0921-5093(02)00408-2 .

[28] Xiang Wu, Ziyu Wu, Lin Guo, Chenmin Liu, Jing Liu, Xiaodong Li, Huibin Xu, Pressure-induced phase transformation in controlled shape ZnO nanorods, Solid State Communications, 135(11), 2005,780-784, https://doi.org/10.1016/j.ssc.2005.02.011.

[29] R. Seelaboyina, N. Phatak, R. P. Gulve, H. P. Leirmann, and S. K. Saxena, "Thermal expansion of nanocrystalline titanium dioxide (TiO2), zinc oxide (ZnO), nickel oxide (NiO)", Thermal Conductivity, vol. 27, pp. 647–666, 2005.

[30] Y.Q. Liu, H.T. Cong, W. Wang, C.H. Sun, H.M. Cheng, AlN nanoparticle-reinforced nanocrystalline Al matrix composites: Fabrication and mechanical properties, Materials Science and Engineering: A,505(1), 2009, 151-156, https://doi.org/10.1016/j.msea.2008.12.045.

[31] Mahesh Bhagwat, Veda Ramaswamy, Synthesis of nanocrystalline zirconia by amorphous citrate route: structural and thermal (HTXRD) studies, Materials Research Bulletin, 39(11), 2004, 1627-1640, https://doi.org/10.1016/j.materresbull.2004.05.008 .